Int. J. Bio-Inorg. Hybr. Nanomater., 11(4): 179-192, Winter 2022

Density functional theory study of adsorption of acid red 33 Dye on the single-walled BN nanotubes

T. Mansori[1], N. Farhadyar[1] F. Azarakhshi[1]*

[1] *Department of Chemistry, Varamin-Pishva Branch, Islamic Azad University, Varamin, Iran*

Received: 29 June 2022; Accepted: 31 August 2022

ABSTRACT: In this study interaction of acid red 33 Dye with (4, 4) armchair open-end boron nitride nanotubes (BNNTs) in interaction (with a length of 7 Å) was investigated. The impacts of the estereoelectronic effect associated with donor-acceptor electron delocalizations, dipole-dipole interactions and total steric exchange energies on the structural and electronic properties and reactivity of semiconductors of (4, 4) armchair open-end boron nitride nanotube (BNNT) in interaction with acid red 33 Dye was studied based on the Density Functional Theory (DFT) calculations by using the B3LYP/(6-31G, 6-31G* and 6-31+G*) level of theory in gas phase and water solution. Thermodynamic functional analysis indicate that the relative energies (ΔE), free Gibbs energies (ΔG) and enthalpies (ΔH) are negative for (BNNT - acid red 33 Dye) system but the calculated entropies (ΔS) are Positive, suggesting thermodynamic favourability for covalent attachment of Dye on (4, 4) BNNT and this results confirm the structural stability of the BNNT - acid red 33 Dye in both gas and solvent phases. Delocalization of charge density between the bonding or lone pair and antibonding orbitals calculated by NBO (natural bond orbital) analysis. These methods are used as a tool to determine structural characterization BNNTs during the adsorption reactions in the gas phase. In order to investigation of conductivity and electronic properties of (4, 4) open-end boron nitride nanotube (BNNT) in the reaction with acid red 33 Dye, the total electronic energy, dipole moment, orbital energies, charge density, density of state (DOS), energy bond gaps, Adsorption energies (E_{Ad}), the global index were calculated. The calculated LUMO-HOMO energy bond gap show that charge density transfer occurs within the molecules and the semi-conductivity of BNNTs could be justified.

Keywords: *Acid red 33 Dye, BNNTs, Density functional theory (DFT), Energy gap, NBO, Semiconductor.*

INTRODUCTION

One of the major industries polluting the environment is industrial effluents. Textile and Dyeing industries are one of the important and basic industries and are considered as one of the indicators of the development of any country. Other industries, such as cosmetics, leather-making, pharmaceutical, paper-making, and paint factories, also produce colored wastewater [1]. Due to the limitation of water resources and the increasing expansion of industrial units, the increase in the production of industrial wastewater and the pollution of water sources are considered environmental problems. Among different pollutants, Dyes are among inorganic and especially organic compounds that are produced all over the world in various parts of human daily life [1]. Dyes are aromatic organic compounds that absorb

(*) Corresponding Author - e-mail: diamond4far@gmail.com

light at a wavelength of 350-700 nm (visible light) and are considered as one of the basic environmental problems. Colors based on chemical structure into 20-30 major groups such as; Acidic, alkaline, active, dispersed, azo, diazo and metallic Dyes are divided [2]. Azo Dyes can be mentioned among the Dyes used in various industries. These Dyes are one of the largest group of synthetic Dyes and can be identified with one or more azo bonds (-N=N-) [3]. Azo Dyes mainly have one or more benzene rings. Due to their toxicity and indestructibility, if they enter the environment without treatment, they can cause irreparable damage to the environment [4]. The discharge of Dyed effluents into lakes and rivers reduces light transmission, reduces the amount of dissolved oxygen and increases the chemical oxygen demand, thus disrupting the life of aquatic animals. In addition, researchers have found that some Dye compounds can produce carcinogenic aromatic amines during the reduction process. Therefore, without complete and proper purification, these compounds are able to remain in the environment for a very long time and in a stable manner [5, 6]. Colored compounds have resistant and complex structures, for this reason their removal using biological methods is difficult and requires a long time and controlled conditions.

Nano adsorbents are widely used as separator filters in water purification and to remove inorganic and organic pollutants from polluted water. Nanoparticles have two key properties that make their use as adsorbent attractive. They have much larger surface areas than bulk particles. Also, nanoparticles can be combined with different chemical groups to increase the ability to remove target compounds. Vast researches and advances are being made in the world to identify the applications of carbon nanotubes in the water and sewage industry, but the theoretical studies conducted in relation to the ability of carbon nanotubes, including boron nitride nanotubes, in removing color have been very limited. The surface absorption process is the most widely used recent technology for color removal due to being cheaper and more effective than other technologies. Especially when these elements are present in low concentrations in water and many materials in wastewater, surface absorption process has been used. Carbon nanotubes and BNNT nanotubes have exceptional absorption capacity and high efficiency in removing various pollutants. Researches have shown that these substances can be a good absorbent in removing color from water-polluting industries' effluents, including Dye and textile industries [7-14]. The prediction of the carbon nanotubes (CNTs) by [15], which can be metallic or semiconductor in character, depending on their chirality and their diameter; CNTs have recently revealed as materials of different properties and various applications in gas storage, sensors and in environment applications. In 1994 [16] theoretically suggested the existence of the boron nitride nanotubes (BNNTs), which were synthesized, by [17] BNNTs possess excellent mechanical properties, high thermal conductivity, chemical stability; unique properties including tensile strength, stiffness and deformation are the features of BNNTs, and resistance to the oxidation, among other properties. Boron nitride nanotube (BNNT) has unique properties of semiconductor behaviour. BNNT has a smaller band gap of a material that is interesting for applications in nanoscale devices. Previously adsorption of different molecules toward nanostructures has been studied [18-25]. There is sufficient published experimental information about the Dye removal from textile wastewater but there is no quantitative theoretical published data about the electronic properties and reactivity of boron nitride nanotube (BNNT) as separator filters in water purification. Because nowadays humans use computer simulation to save time and money to achieve accurate calculation results and then incurs research and laboratory costs. In this project, the computer simulation of the process of carrying out a reaction using modern computing methods is discussed. The applied theory of electron density function has become a powerful and informative tool to study the reactivity of organic molecules and to describe intermolecular interactions. The energy of a molecule is determined only by a function of the electron density. The purpose of this study is to know the sites or atoms responsible for the absorption of dye molecules on the absorbent surface [22-26].

In this study, (4, 4) armchair BNNT have been carried out to adsorption of 7-hydroxy phenothiazine 3-one Dye as environmental pollution by DFT method. Also, the stabilization energies (E_2) associated

with electronic delocalization and their influences on the structural properties of azo Dye-BNNT were quantitatively investigated by the NBO (Natural Bond Orbital) analysis [26]. The resonance energies (LP→ σ* or π*) are proportional to $S^2/\Delta E$ where S is the orbital overlap and ΔE is the energy differences between the donor and acceptor (LP and σ* or π*) orbitals [27, 28]. We have investigated frontier molecular orbitals, quantum-chemical molecular descriptors, MEP analysis, chemical shift tensors, and charge transfer analysis according to NBO analysis.

COMPUTATIONAL DETAILS

The main goal of the research was to measure and evaluate the effects of electron destabilization, steric repulsions and dipole-dipole interactions on the structural and electronic properties and reactivity of the structures of acid red 33 Dye (C16H13N3O7S2) and armchair boron nitride nanotube (4,4) (B24N24H16). It is a single wall with a length of 7 angstroms. The used methods are a tool to determine the structural characteristics in gas phase and solvent phase. DFT electron density functional theory quantum mechanical calculations and molecular orbital calculations at B3LYP/6-31G* theoretical levels in order to minimize the energy of the structures of acid red 33 Dye and boron nitride nanotube (4,4) (B24N24H16) alone and in the presence of each other. The structures of BNNT-acid red 33 Dye (C16H29B24N27O7S2) was optimized at the B3LYP/6-31G* level of theory by using Gaussian quantum chemical package [29]. The B3LYP is commonly used functional in the study of different nanostructures method [30]. The vibrational frequencies have been calculated at the same level of theory, which enable us to confirm real minima. The acid red 33 Dye molecules have been sat in different sites to be close to the BNNT (Fig. 1). The Adsorption energies (E_{Ad}) of acid red 33 Dye on the BNNT are determined through the following equation (1):

$$\Delta E_{adsorption} = E(Dye-BNNT) - [E(Dye) + E(BNNT)] \quad (1)$$

Where E(Dye – BNNT) is the total energy of the BNNTs interacting with Dye, E(Dye) and E(BNNT) are total energies of the pure BNNT and Dye respectively. NBO analysis was then performed using the B3LYP/6-31G* level for the adsorption interaction of acid red 33 Dye on the BNNT by the NBO analysis [27, 28]. The molecular orbital (MO) calculations of the investigated compounds such as EHOMO, ELUMO, energy gap between LUMO and HOMO (Eg = ELUMO – EHOMO) were also performed. The optimized molecular structures, HOMO, LUMO and MEP surfaces were visualized using GaussView 05 program [28]. The electronic structure of the mentioned compounds was also studied by using NBO analysis at the B3LYP/6-31G* level of theory in order to understand hyperconjugative interactions and charge delocalization in the Dye molecule and the Dye/BNNT(4,4) complex.

RESULTS AND DISCUSSION

Optimized Structures

At first, the Dye and BNNT(4,4) molecules and Dye/BNNT(4,4) complex have optimized using B3LYP/6-31G* level of theory in the gas phase and solvent (water) phase. The optimized structures of the Dye, BNNT(4,4) compounds and Dye/BNNT(4,4) com-

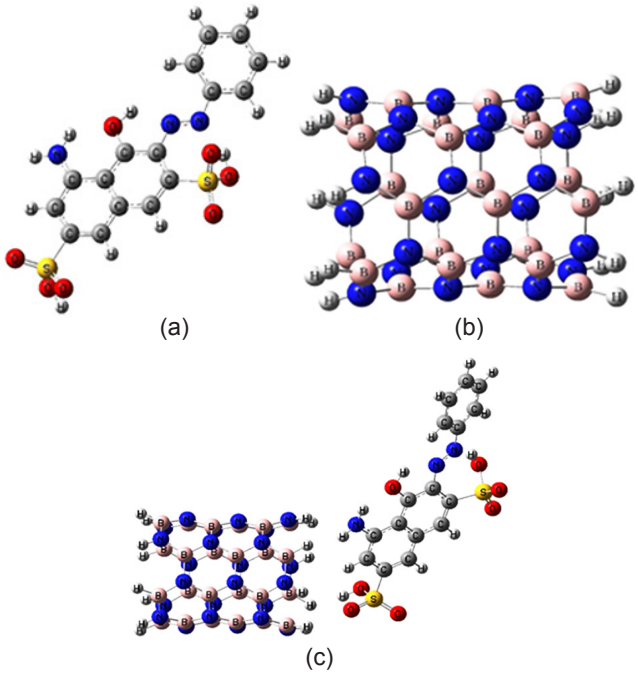

Fig. 1. The optimized geometry of the acid red 33 Dye (a), the BNNT(4,4) (b) and Dye/BNNT(4,4) complex (c) using B3LYP/6-31G* level of theory.

Table 1. The calculated adsorption energy (Ead) values of the Dye molecule over the BNNT(4,4) in gas and solvent phase using B3LYP/6-31G* level of theory in kcal/mol.

SCF done energy (kcal/mol) in gas phase			Adsorption Energy
Dye – $B_{24}N_{24}H_{16}$	Dye	$B_{24}N_{24}H_{16}$	$\Delta E_{adsorption}$
-2527077.221	-1320637.428	-1206434.268	-5.525
SCF done energy (kcal/mol) in solvent phase			Adsorption Energy
Dye – $B_{24}N_{24}H_{16}$	Dye	$B_{24}N_{24}H_{16}$	$\Delta E_{adsorption}$
-2527079.499	-1320639.461	-1206434.27	-5.768

plex are shown in Fig. 1. According to Table 1, the calculated adsorption energy (E_{ad}) values of the molecule Dye over the BNNT(4,4) in the gas and water phase are -5.525 kcal/mol, -5.768 kcal/mol, respectively; therefore, the interaction in the gas and solvent phases is exothermic (Table 1). The highest adsorption energy and a strong chemisorption is observed in the water solvent (-5.768 kcal/mol) compared with gas phase and Thus in following, the calculations carried out in the water solvent.

Tables 2-5 shows the thermochemical parameters such as the sum of electronic and thermal energies (E+T), sum of electronic and thermal enthalpies (E+H), sum of electronic and thermal free energies (E+G), zeropoint energy (ZPE), sum of electronic and zeropoint energies (E+ZPE), electronic energy (E) and entropy (S) of the compounds Dye, the BNNT(4,4) , and the complex Dye/BNNT(4,4) optimized using B3LYP/6-31G* level of theory in the gas phase and solvent water. According to the results in Tables 2-5, with the adsorption of the molecule Dye on BNNT(4,4), the Thermal, Gibbs, Enthalpy and E+ZPE energies values decrease in both gas and solvent phase. Energy values reflect the reduced reactivity and increase the stabil-

Table 2. The calculated thermochemical parameters of the molecules Dye, BNNT(4,4) and complex Dye/BNNT(4,4) by B3LYP/6-31G* level of theory in gas phase in kcal/mol.

Compounds	$G+E_{el}$	$H+E_{el}$	$E_{thermal}+E_{el}$	E_0= ZPE+Eel	ZPE	S
Dye	-1320491.672	-1320445.110	-1320445.702	-1320459.293	178.135	0.156
BNNT	-1206220.746	-1206172.339	-1206142.696	-1206191.238	243.030	0.162
Dye –BNNT	-2526721.871	-2526623.457	-2526593.804	-2526659.488	417.733	0.308

Table 3. The thermodynamic parameters differences in gas phase in kcal/mol / at B3LYP/6-31G*.

ΔG	ΔH	ΔS	ΔE_0	$\Delta E_{thermal}$
-9.452	-6.008	-0.010	-8.957	-5.406

Table 4. The calculated thermochemical parameters of the molecules Dye, BNNT(4,4) and complex Dye/BNNT(4,4) by B3LYP/6-31G* level of theory in the solvent phase in kcal/mol.

Compounds	$G+E_{el}$	$H+E_{el}$	$E_{thermal}+E_{el}$	E_0= ZPE+Eel	ZPE	S
Dye	-1320494.930	-1320442.705	-1320443.297	-1320458.945	180.516	0.175
BNNT	-1206195.841	-1206143.067	-1206143.660	-1206162.575	271.693	0.177
Dye –BNNT	-2526700.656	-2526592.403	-2526592.871	-2526630.731	448.768	0.281

Table 5. The thermodynamic parameters differences in solvent phase in kcal/mol / at B3LYP/6-31G*.

ΔG	ΔH	ΔS	ΔE_0	$\Delta E_{thermal}$
-9.885	-6.631	-0.072	-9.211	-5.913

ity of Dye in non-bonded interaction with BNNT(4,4). The thermodynamic parameters values in the solvent water are more negative compared with the gas phase. Therefore, the complex Dye/BNNT(4,4) in the solvent water is more stable rather than the gas phase.

IR Spectrum

The calculated IR spectra of Dye, BNNT and Dye/BNNT complex is studied using B3LYP/6-3G* level of theory (Figs. 2-4). The important peaks of IR spectra of the acid red 33 Dye: is observed at: In the region υ= 3745 cm^{-1} the stretching vibration frequency related to the O-H bond attached to the aromatic ring has appeared. In the areas of υ= 3173 cm^{-1} and υ= 3223 cm^{-1} symmetric and asymmetric stretching vibration frequencies of C-H bonds related to (C=C-H) aromatic hydrocarbons have appeared. In the area of υ= 1721 cm^{-1} the stretching vibration frequency of the C=O carbonyl group attached to the aromatic ring has appeared. Two moderate peaks appeared in the area of υ= 1679 cm^{-1} and υ= 1657 cm^{-1} which are related to the stretching vibrations of the C=N double bond of the

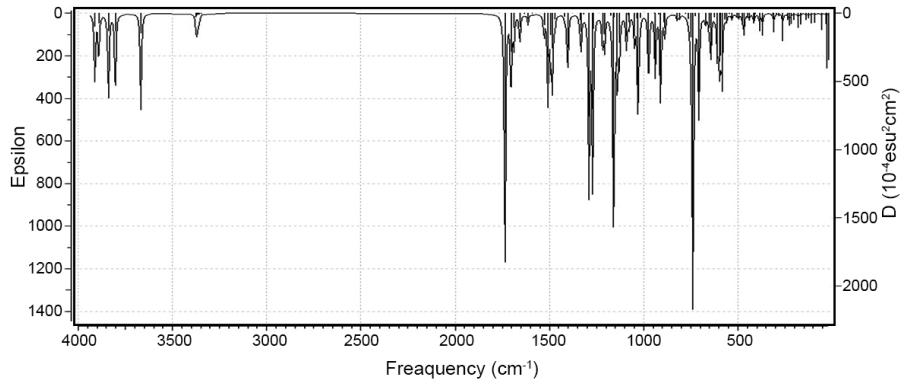

Fig. 2. The IR spectrum of Dye.

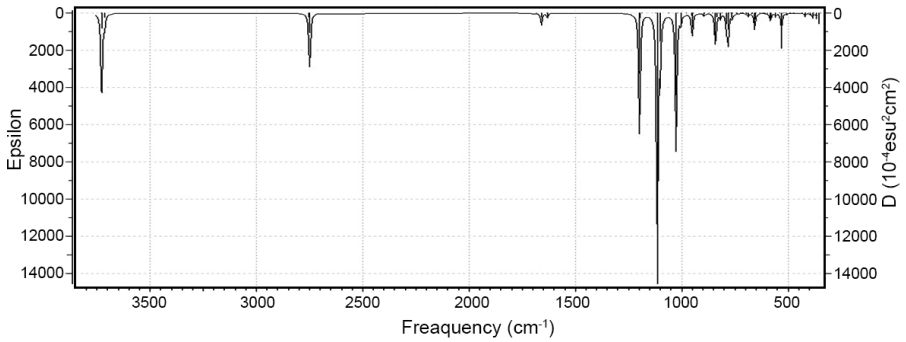

Fig. 3. The IR spectrum of BNNT(4,4)

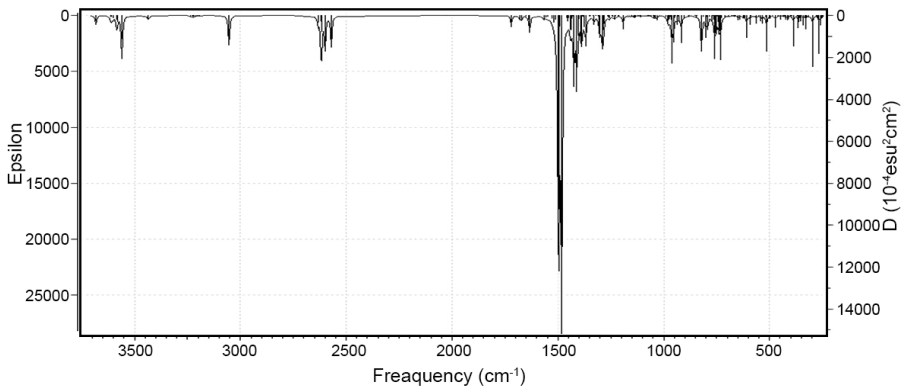

Fig. 4. The IR spectrum of Dye/BNNT(4,4) complex

middle color rings. The peaks that appeared in the area of υ= 1594 cm^{-1} and υ= 1572 cm^{-1} are related to the stretching vibrations of aromatic C=C double bonds. C-H bending vibration frequency of aromatic hydrocarbons appeared in the area of υ= 1475 cm^{-1} and υ= 1389 cm^{-1}. The peaks that appeared in the region of υ= 1331 cm^{-1}, υ= 1308 cm^{-1}, and υ= 1284 cm^{-1} are related to the stretching vibration of C-N and C-S bonds. The frequency of stretching vibrations of C-O and C-C central bonds appeared sharp in the area of υ= 1246, 1216, and 1133 cm^{-1}. Several peaks appeared in the regions of υ= 848, 878 and 893 cm^{-1} and are related to the out-of-plane bending vibration frequencies of C-H in aromatic hydrocarbons. Two sharp peaks appeared in υ= 400 and 409 cm^{-1} and correspond to the bending vibration frequencies of C-N and C-S bonds.

The important peaks of IR spectra of the BNNT(4,4) is observed at :

In the area of υ= 3603 cm^{-1} the stretching vibration frequency related to N-H bonds has appeared. In the region of υ= 2628 cm^{-1} the stretching vibration frequency related to B=N bonds has appeared. The long and sharp peak that appeared in the area of υ= 1498 cm^{-1} is related to the stretching vibrations of B–N–B bonds. In the region of υ= 1443 cm^{-1}, υ= 1410 cm^{-1} and υ= 1333 cm^{-1} the bending vibrations of N-H bonds have appeared. In the region υ= 780 cm^{-1} and υ= 693 cm^{-1} the frequencies of bending vibrations of B–N–B bonds have appeared.

The important peaks of IR spectra of the Dye/ BNNT(4,4) complex is observed at :

In the IR spectrum related to the dye-boron nitride nanotube complex, the frequencies of stretching and bending vibrations are as follows: In the area of υ= 3743 cm^{-1} the stretching vibration frequency related to the N-H bond of boron nitride nanotubes has appeared. In the area of υ= 3605 cm^{-1} the stretching vibration frequency related to the O-H bond of the dye molecule has appeared. In the regions of υ= 3173 cm^{-1} and υ= 3219 cm^{-1} weak peaks for symmetric and asymmetric stretching vibrations of C-H bonds related to (C=C-H) aromatic hydrocarbons have appeared. In the area of υ= 2622 cm^{-1} the stretching vibration frequency related to B=N bonds has appeared. In the area of υ= 1706 cm^{-1} the stretching vibration frequency of the C=O carbonyl group attached to the aromatic ring has appeared. Two moderate peaks appeared in the area of υ= 1676 cm^{-1} and υ= 1656 cm^{-1} which are related to the stretching vibrations of the C=N double bond of the middle color rings. The peaks that appeared in the area of υ= 1568 cm^{-1} and υ= 1591 cm^{-1} are related to the stretching vibrations of aromatic C=C double bonds. The long and sharp peak that appeared in the region of υ = 1500 cm^{-1} is related to the stretching vibrations of B–N–B bonds. In the region of υ= 1444 cm^{-1} and υ= 1409 cm^{-1} and υ= 1370 cm^{-1} the bending vibrations of N-H bonds have appeared. C-H bending vibration frequency of aromatic hydrocarbons has appeared in the area of υ= 1331, 1312 cm^{-1}. In the area of υ= 1280 cm^{-1}, the broad peak that appears is related to the stretching vibrations of C-N and C-S bonds. The frequency of stretching vibrations of C-O bonds in the area of υ= 1210 cm^{-1} has appeared as a broad and sharp peak. The frequency of stretching vibrations of C-C bonds appeared in the region of υ= 1135, 1028 and 1028 cm^{-1}. Several peaks appeared in the regions of 922, 880 and 848 cm^{-1} and correspond to the out-of-plane bending vibration frequencies of C-H in (C=C-H) aromatic hydrocarbons. In the areas of υ= 780, 696 and 680 cm^{-1} the frequencies of bending vibrations of B–N–B bonds have appeared. Two sharp peaks appeared in the regions of υ = 494 and 402 cm^{-1} and correspond to the bending vibration frequencies of C-N and C-S bonds.

NBO Analysis

NBO analysis is an important method for studying intra- and inter-molecular bonding and interaction between bonds in molecular systems [31]. The electron delocalization from donor orbitals (full NBOs) to acceptor orbitals (empty NBOs) describes a conjugative electron transfer process between them [29]. For each donor orbital (i) and acceptor orbital (j), the stabilization energy E(2) associated with the delocalization i → j is computed [32]:

$$E_2 = q_i \frac{F^2(i,j)}{E_j - E_i} \quad (2)$$

The stabilization energy (E(2)) describes the amount of the participation of electrons in the resonance be-

tween atoms of the molecular system [29]. The bigger E(2), the more donation tendency from electron donors to electron acceptors. The NBO analysis for Dye/BNNT(4,4) complex has been carried out by B3LYP/6-31G* level of theory in the water solvent and the results are summarized in Table 4. According to results of NBO analysis for the red acid 33-boron nitride nanotube complex, the highest resonance energies due to electron destabilization BD(1) B14-H53→BD*(1)O80-H99 (E2=7.59 kcal/mol) and BD(1) B38-H61→BD*(1)N75-H97 (E2=2.49 kcal/mol) which are related to Electron destabilization from boron nitride nanotube to Dye (Table 6). Also, other resonance energies resulting from electron destabilization from boron nitride nanotube to Dye are: BD(1)B7-N15→BD*(1)O80-H99, BD(1)B14-N15 →BD*(1)O80-H99 , BD(1)N16-B17→BD*(1)O80-H99, BD*(2)B14-N15→BD*(1)O80-H99 and the resonance energies due to electron destabilization are: 0.06, 0.06, 0.10, 0.07 kcal/mol respectively. Also, for the dye-boron nitride nanotube complex, the highest resonance energy is due to electronic destabilization from the dye to the boron nitride nanotube LP(1)N75 →BD*(1)N46-H64 (E2=2.04 kcal/mol) and others Resonance energies from dye to boron nitride nanotube are:
BD(1)N75-H96→BD*(1)B38-H61, BD(1)N75-H97→BD*(1)B38-H61, BD(1)N75-H97→BD*(1)N46-H64, BD(1)O80-H99→BD*(1)B14-N16, BD(1)O80-H99→BD*(1)B14-H53, LP(1)O78→BD*(1)N22-H56, LP(1)O78→BD*(1)B30-N32, LP(2)O78→BD*(1)N22-H56, LP(3)O78→BD*(2)B14-N15, LP(3)O78→BD*(1)N22-H56, LP(1)O80→BD*(1)B14-H53, LP(2)O80→BD*(1)N15-H54, BD*(1)S77-O78→BD*(1)N22-H56, and the resonance energies due to electron destabilization are: 0.06, 0.50, 0.18, 0.16, 0.51, 0.92, 0.09, 0.12, 0.08, 0.63, 0.19, 13 0.0 and 0.35 kcal/mol respectively (Table 6). The total resonance energy (stability) caused by electronic destabilization from the boron nitride nanotube to the dye (10.37) is more than the destabilization of the electron from the dye to the boron nitride nanotube (5.96). The stability of the complex (dye - boron nitride nanotube) increases by increasing the electron resonance from the drug to the nanotube and the boron nitride nanotube to the dye. So, Dye

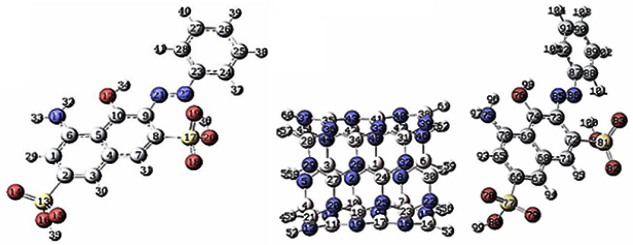

(a) (b)

Fig. 5. Numbering of atoms in the optimal structures (a) acid red 33 Dye and acid red 33 - boron nitride nanotubes complex (b).

and BNNT(4,4) acts as both electron donor and electron acceptor; therefore, charge transfer takes place between Dye and BNNT(4,4) in the complex Dye/BNNT(4,4). Thus there are the most important donor–acceptor interactions between the molecule Dye and BN nanotube.

NBO calculations show (Fi,j) values for electron delocalization BD(1) B14-H53→BD*(1)O80-H99, BD(1) B14-H53→BD*(1)O80-H99 (E2= 7.59) and BD(1) B38-H61→BD*(1)N75-H97 (E2=49/2) and LP(1)N75→BD*(1)N46-H64 (E2= 2.04) in dye-boron nitride nanotube complex calculated 0.071, 0.042 and 0.037 (a.u.) respectively. By comparing the numerical value of Fi,j (the amount of orbital overlap) obtained for electron transitions (Table 6), it can be said that the increase in the amount of orbital overlap justifies the increase in resonance energies due to electron destabilization. Considering that the calculations of thermodynamic functions and the amount of Gap's free energy differences (ΔG) and enthalpy differences (ΔH) of the reaction calculated in the gas phase and the solution phase justify the exothermic nature of the reaction, based on the results of NBO analysis, Stereoelectronic effects caused by electron destabilization are also successful in increasing the stability of boron nitride nanotube-dye complex.

According to the Boltzmann distribution law, the greater the population difference between the donor and acceptor molecular orbitals, the better the electron transfer is performed, if the population difference is small or equal, it is a saturation state and electron transfers are not performed well. When red acid 33 is placed in the presence of boron nitride nanotube, for electron transfer BD(1) B14-H53→BD*(1)O80-H99 with the highest resonance energy (E2=7.59 kcal/

Table 6. Resonance energies (E(2)/kcal/mol), energy difference of orbitals (ΔE= E(j)-E(i), a.u.), degree of orbital overlapping (off diagonal elements in the matrix) (Fij, a.u.), boron nitride-acid red 33 complex using DFT calculations at the B3LYP/6-31G* level of theory.

Second Order Perturbation Theory Analysis of Fock Matrix in NBO Basis			
Donor NBO (i) Acceptor NBO (j)	E(2)/ kcal/mol	E(j)-E(i)/ a.u.	F(i,j)/ a.u.
from unit 1(BNNT) to unit 2(Dye)			
BD (1) B7 - N15 ⟶ BD*(1) O80 - H99	0.06	1.09	0.007
BD (1) B14 - N15 ⟶ BD*(1) O80 - H99	0.06	1.09	0.007
BD (1) B14 - H53 ⟶ BD*(1) O80 - H99	7.59	0.83	0.071
BD (1) N16 - B17 ⟶ BD*(1) O80 - H99	0.10	1.06	0.009
BD (1) B38 - H61 ⟶ BD*(1) N75 - H97	2.49	0.88	0.042
BD*(2) B14 - N15 ⟶ BD*(1) O80 - H99	0.07	0.33	0.015
Σ	10.37		
from unit 2(Dye) to unit 1(BNNT)			
BD (1) N75 - H96 ⟶ BD*(1) B38 - H61	0.06	1.16	0.007
BD (1) N75 - H97 ⟶ BD*(1) B38 - H61	0.50	1.16	0.021
BD (1) N75 - H97 ⟶ BD*(1) N46 - H64	0.18	1.14	0.013
BD (1) O80 - H99 ⟶ BD*(1) B14 - N16	0.16	1.25	0.013
BD (1) O80 - H99 ⟶ BD*(1) B14 - H53	0.51	1.27	0.023
LP (1) N75 ⟶ BD*(1) N46 - H64	2.04	0.77	0.037
LP (1) O78 ⟶ BD*(1) N22 - H56	0.92	1.29	0.031
LP (1) O78 ⟶ BD*(1) B30 - N32	0.09	1.26	0.009
LP (2) O78 ⟶ BD*(1) N22 - H56	0.12	0.79	0.009
LP (3) O78 ⟶ BD*(2) B14 - N15	0.08	0.37	0.005
LP (3) O 78 ⟶ BD*(1) N22 - H56	0.63	0.79	0.021
LP (1) O80 ⟶ BD*(1) B14 - H53	0.19	1.16	0.013
LP (2) O80 ⟶ BD*(1) N15 - H54	0.13	0.82	0.009
BD*(1) S77 - O78 ⟶ BD*(1) N22 - H56	0.35	0.22	0.026
Σ	5.96		

mol), the electron population difference between the molecular orbitals of donor BD(1)B14-H53 (1.96735) and electron acceptor BD*(1)O80-H99 (0.02654), is high and according to Boltzmann's law, electron transfer is carried out well.

Atomic charge

The Mulliken atomic charge distribution of red acid 33 and boron nitride nanotube alone and in the presence of each other (in complex) was calculated at the B3LYP/6-31G* level of theory, and the obtained results show that the charge density changes on the atoms involved in the reaction of Dye and BNNT (4.4) The calculated natural charges for selected atoms in these molecular systems are summarized in Table 7 (atoms are numbered according to Fig. 5). The most significant changes in the Mulliken atomic charges observed for C68, C70, C73, O76, S77, O78, O80, S81, N85, C87 atoms because of Dye in the complex Dye/BNNT(4,4) is close to these atoms in the BN nanotube (Fig. 6).

Electrostatic potential of the molecule

One of the useful features for studying reactivity is determining the molecular electrostatic potential. The molecular electrostatic potential (MEP) shows that the area with the most negative charge is red and is a suitable place for the attack of the electrophilic molecule. Also, the area with the most positive charge is blue and is a suitable place for the attack of nucleophilic molecules. (MEP) is important in the sense that in order to show the size of the molecule, the shape of the molecule is used as centers with negative and positive electrostatic potential, as a color range. In general, the

Table 7. Mulliken atomic charge distribution calculated for Dye alone and in the presence of boron nitride nanotube.

Mulliken atomic charge / B3LYP/6-31G*				
Within (Dye)		Within (Dye) in Dye-BNNT		Δq
1 C	-0.2138	65 C	-0.2124	0.0013
2 C	-0.1547	66 C	-0.1558	0.0011
3 C	-0.2427	67 C	-0.2206	0.0221
4 C	0.1675	68 C	0.1382	0.0293
5 C	0.0941	69 C	0.0863	0.0078
6 C	0.3475	70 C	0.3125	0.0350
7 C	-0.2505	71 C	-0.2396	0.0108
8 C	-0.1808	72 C	-0.1975	0.0168
9 C	0.2544	73 C	0.3317	0.0772
10 C	0.2811	74 C	0.2663	0.0147
11 N	-0.8476	75 N	-0.8448	0.0027
12 O	-0.7036	76 O	-0.6677	0.0359
13 S	1.1604	77 S	1.2110	0.0506
14 O	-0.4898	78 O	-0.5410	0.0511
15 O	-0.5042	79 O	-0.4796	0.0246
16 O	-0.6190	80 O	-0.6665	0.0474
17 S	1.2977	81 S	1.2353	0.0623
18 O	-0.4928	82 O	-0.4970	0.0042
19 O	-0.5261	83 O	-0.5082	0.0178
20 O	-0.6588	84 O	-0.6642	0.0054
21 N	-0.3108	85 N	-0.3871	0.0763
22 N	-0.4001	86 N	-0.4052	0.0051
23 C	0.2673	87 C	0.3268	0.0595
24 C	-0.1367	88 C	-0.1545	0.0178
25 C	-0.1388	89 C	-0.1367	0.0020
26 C	-0.1110	90 C	-0.1142	0.0032
27 C	-0.1389	91 C	-0.1415	0.0025
28 C	-0.1342	92 C	-0.1306	0.0036

nucleophilic and electrophilic sites in a molecule are determined by (MEP) and it is possible to predict the active sites to participate in the reaction. In the mixture of acid red 33-boron nitride nanotubes, the positive

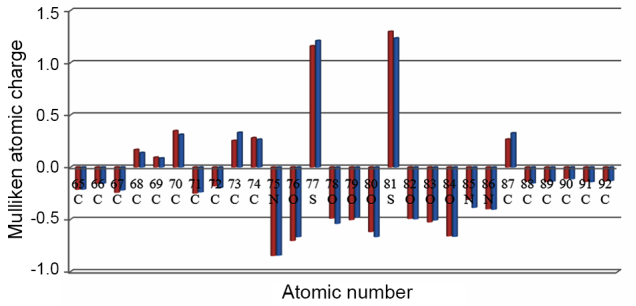

Fig. 6. Mulliken diagram of atomic charge on drug atoms alone and drug in the presence of boron nitride nanotube.

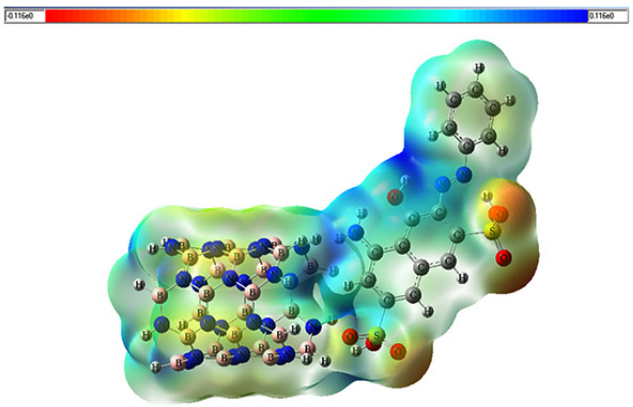

Fig. 7. A diagram of the molecular electrostatic potential (MEP) calculated by the self-consistent field theory (SCF) for acid red 33- boron nitride nanotubes, a system with 105 atoms and 522 electrons, neutral and in the ground state.

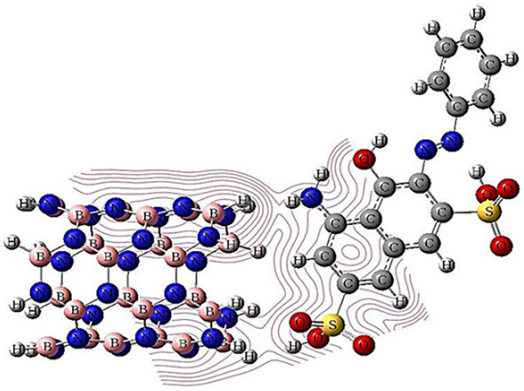

Fig. 8. Contour lines showing the range of atoms involved in electron resonance in the absorption reaction of red acid molecule 33 on boron nitride nanotube (4.4) with a length of 7 angstroms.

charge density is dominant on the atoms of the dye, which by electron resonance direct the charge density towards the reaction center (oxygen of the sulfonyl group) and are far from the reaction center, and the charge density is The negative is dominant on the oxygen atoms of sulfonyl groups of acid red 33, which was involved in the reaction, and in this way, the reactive centers in this complex are determined (Fig. 7). In Fig. 8, the Contour lines show that in the reaction of dye molecule absorption on boron nitride nanotube, in which part of red acid dye 33 and boron nitride nanotube, electron interaction is taking place.

Electronic Properties

The frontier molecular orbitals (FMO) including HOMO and LUMO are indicated as significant parameters for the chemical reactions [29]. The HOMO and LUMO energies represent the ability to donate an electron and obtain an electron respectively. The molecular orbitals have a significant role in charge transfer phenomenon in molecular systems. The energy gap between HOMO and LUMO orbitals is an important factor in determining electrical transport properties in molecular systems [29]. We have investigated the non-bonded intermolecular interaction effects between the molecule Dye and BNNT(4,4) on the electronic properties. The calculated results are reported in Table 5.

After the adsorption of the molecule Dye over BNNT(4,4), the energies of HOMO and LUMO are decreased from -5.9796 eV and -3.2392 eV in the molecule Dye to -6.0495 and -3.3692 eV respectively, in

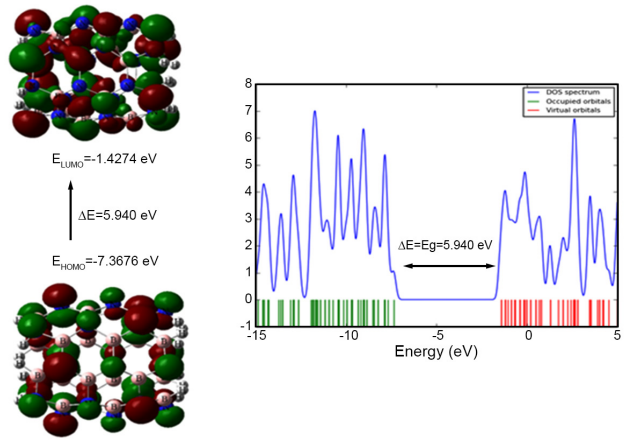

Fig. 10. The calculated HOMO, LUMO orbitals of the BNNT(4,4) molecule and the computed DOS plot of the molecules.

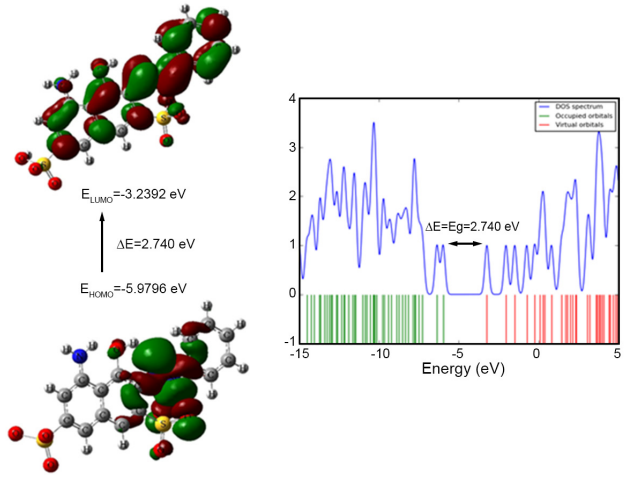

Fig. 9. The calculated HOMO, LUMO orbitals of Dye molecule and the computed DOS plot of the molecules.

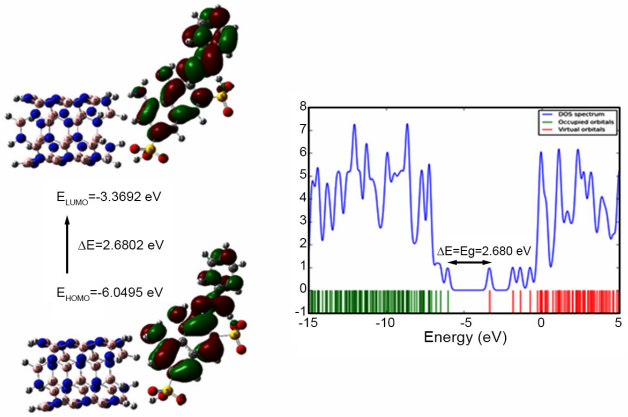

Fig. 11. The calculated HOMO, LUMO orbitals of Dye/BNNT(4,4) complex and the computed DOS plot of the molecules.

the complex Dye/BNNT(4,4). The energy of HOMO is increased from -7.3676 eV in the BNNT(4,4) to -6.0495 eV in the complex Dye/BNNT(4,4), whereas the energy of LUMO is decreased from -1.4274 eV to -3.3692 eV. Figs. 9-11 show the energy gap of HOMO and LUMO molecular orbitals as well as the DOS diagram. The frontier orbitals graphs of the Dye and BNNT(4,4) molecules show that the electron density of HOMO orbital in the BNNT(4,4) is mainly situated on nitrogen atoms, whereas the LUMO orbital is localized on boron atoms. The electron density of LUMO orbital in the molecule Dye is mainly localized on the whole molecule and the HOMO orbital is spread over the middle part of structure. The HOMO and LUMO orbitals of the Dye/BNNT(4,4) complex focus only on the molecule Dye. It is predicted that the possibility of reaction with electrophilic species is in the part where the distribution of HOMO orbitals is more, and the possibility of reaction with nucleophilic species is in the side where the distribution of LUMO orbitals is more. Computed DOS plots in Figs. 9-11 show the energy gaps of the Dye and BNNT(4,4) molecules and Dye/BNNT(4,4) complex. The energy gaps values of the title molecular systems is also reported in Table 5. The energy gap between LUMO and HOMO (Eg) of Dye is 2.7404 eV and after the adsorption of Dye over BNNT(4,4) is decreased to 2.6802 eV. Also, the energy gap is decreased from 5.9402 eV in BNNT(4,4) to 2.6802 eV in the complexe Dye/BNNT(4,4). These results show a significant increase in electrical conductivity of the system complex Dye/BNNT(4,4) compared with the isolated Dye and BNNT(4,4) Figs. 9-11. On the other hand, the reactivity of a molecule is related to its energy gap. The energy gap of molecular orbitals (ELUMO-EHOMO energy gaps) shows that a soft molecule has a small energy gap and a hard molecule has a large energy gap. Stabilizing orbital interactions increase by decreasing the energy level of the electron acceptor orbital and increasing the energy level of the electron donor orbital. In addition, electron destabilization is confirmed by changing the population of electron donor and acceptor orbitals Also, in the boron nitride nanotube dye mixture, with the decrease of the Eg energy gap, the hardness parameter is decreased, the softness parameter is slightly decreased, and the amount of ionization energy and electron-withdrawing energy, as well as the values of electronegativity and electrophilicity, are increased. Such changes in the boron nitride nanotube-dye mixture can be explained through the electron-withdrawing effects of the sulfonyl groups and the electron-donating effects of the hydroxy and amine groups of the dye in the mixture.

Indices of molecular reactivity

DFT method is a useful method to investigate the characteristics of chemical structures based on the reactivity index of molecules. The quantum molecular descriptors for the investigated molecular systems consist of ionization potential (I), electron affinity (A), chemical hardness (η), electrophilicity (w), electronegativity (χ), chemical softness (S), electron chemical potential (μ) and the amount of electron charge transfer (ΔNmax) in the equilibrium state at temperature (T) is calculated based on the following equations [31, 32]:

$$\mu = \frac{(E_{HOMO} + E_{LUMO})}{2} = -\chi \quad (3)$$

$$\eta = \frac{(E_{LUMO} - E_{HOMO})}{2} \quad (4)$$

$$S = \frac{1}{2\eta} \quad (5)$$

$$W = \left(\frac{\mu^2}{2\eta}\right) \quad (6)$$

$$\Delta N_{max} = \frac{-\mu}{\eta}, \qquad \text{inreaction} : \Delta N_{max} = \frac{-(\mu A - \mu B)}{2(\eta A + \eta B)} \quad (7)$$

$$EI = -E_{HOMO} \quad (8)$$

$$EA = -E_{LUMO} \quad (9)$$

The results are reported in Table 8. The stability of the molecular systems is related to hardness which is a tool to understand chemical reactivity [25]. As shown in Table 8, the global hardness of the Dye, BNNT(4,4) molecules and Dye/BNNT(4,4) complex are 1.3702 eV, 2.9701 eV and 1.3401 eV, respectively. After the adsorption of Dye on the BN nanotube, the global hardness value of the Dye/BNNT(4,4) complex

Table 8. Reactivity indices for dye molecule, boron nitride nanotube and mixture of dye molecule - boron nitride nanotube in terms of electron volts.

Electronic Properties / B3LYP/6-31g*	Compounds		
	Dye	BNNT	Dye-BNNT
E_{HOMO} / (eV)	-5.9796	-7.3676	-6.0495
E_{LUMO} / (eV)	-3.2392	-1.4274	-3.3692
Energy gap (Eg) / (eV)	2.7404	5.9402	2.6802
Ionization potential (EI) / (eV)	5.9796	7.3676	6.0495
Electron affinity (EA) / (eV)	3.2392	1.4274	3.3692
Electronegativity (χ) / (eV)	4.6094	4.3975	4.7094
Global hardness (η) / (eV)	1.3702	2.9701	1.3401
Chemical potential (μ) / (eV)	-4.6094	-4.3975	-4.7094
Global electrophilicity (ω) / (eV)	7.7532	3.2555	8.27467
Chemical softness (S)/ (eV^{-1})	0.6851	1.4850	0.6700
Dipole Moment / (Debye)	9.8191	0.00	10.7477
ΔNmax	3.3640	1.4806	3.5141
ΔNmax (in reaction)			0.0244

is decreased rather than isolated Dye and BNNT(4,4). The electrophilicity and electrophilicity values of complex increased compared with isolated Dye and BNNT(4,4). Therefore, the complex Dye/BNNT(4,4) has a high chemical activity, low chemical stability and it is a soft system. Thus, it is found that the adsorption of the molecule Dye on BNNT(4,4) in the solvent phase changes electronic properties of the complex. After Dye adsorption, the dipole moment values of Dye and BNNT(4,4) are increased from 9.8191 and 0.00 respectively, to 10.7477 Debye in complex Dye/BNNT(4,4) (see Table 8). The change of dipole moment after adsorption of Dye over BN nanotube indicates a charge transfer between Dye and the BNNT(4,4). The atomic charges have a significant role on physical properties such as molecular polarizability, dipole moment, electronic structure and related properties of molecular systems [25]. The charge distributions (NBO charges) for equilibrium geometry of the molecules Dye, BNNT(4,4) and complex Dye/BNNT(4,4) were calculated using B3LYP/6-31G* level of theory. Also, the (ΔN) quantity shows the load transfer rate in the system. If (ΔN>0) is positive, it indicates the electron transfer from the nanotube (B) to the dye molecule (as an electron acceptor) (A) and if (ΔN<0) is negative, it indicates the electron transfer from the molecule dye (as an electron donor) (A) to the nanotube (B). The (ΔN) quantity (charge transfer) in the red acid mixed system of boron nitride nanotubes is 0.024. which (ΔN>0) and positive indicates the flow of electrons from the side of the boron nitride nanotube towards acid red 33 and the presence of the electron-withdrawing group in the dye molecule Figs. 9-11.

CONCLUSION

In this work, the adsorption of the acid red 33 (Dye) over the BNNT(4,4) is studied at the B3LYP/6-31G* level of theory. According to the obtained results, adsorption of Dye over the BNNT(4,4) in gas phase and various solvents is an exothermic process and Dye/BNNT(4,4) is a stable complex. The highest adsorption energy was observed in the solvent water (-5.768 eV) compared with gas phase and other solvents. It is found that some geometrical parameters of Dye and BNNT(4,4) are changed after adsorption process due to the formation of intermolecular non-bonded interaction. NBO analysis predicted a charge transfer from the molecule Dye to BN nanotube and from BN nanotube to Dye. The energy gap between LUMO and HOMO in Dye increase after the adsorption Dye on BN nanotube. This result indicates a significant increase in electrical conductivity of complex compared with the isolated Dye and BN nanotube. There-

fore, the investigation of Electronic Behaviour of azo Dye- BNNT can provide valuable information about its structural properties and reactivity of BNNTs in interaction with azo Dyes. The results show it is clearly possible to apply armchair BNNTs as a semiconductor, at the presence of azo Dyes and therefore can potentially be used for azo Dyes adsorbent.

REFRENCES

[1] Couto, S.R. (2009). Dye removal by immobilized fungi. Biotechnol. Adv. 27, 227-235.

[2] Lee, J.W. Choi, S.P. Thiruvenkatachari, R. (2006). Evaluation of the performance of adsorption and coagulation processes for the maximum removal of reactive Dyes. Dyes Pigm., 69, 196-203.

[3] Mahmoodi, N. Arami, M. Yousefi, N. (2006). Photocatalytic degradation of triazinic ring-containing azo Dye (reactive red 198) by using immobilized TiO2 photoreactor: Bench scale study. J. Hazard Material. 133, 113-118.

[4] Hameed, B.H. Ahmad, A. (2009). Adsorption of reactive Dye on palm-oil industry wastes: equilibrium, Kinetic and thermodynamic studies. Desalination, 247, 551-560.

[5] Mostafavi, S.T. Mehrnia, M.R. Rashidi, A.M. (2009). Preparation of nanofilter from carbon nanotubes for application in virus removal from water. Desalination, 238, 271-280.

[6] Emami, F. Tehrani-Bagha, A.R. Gharanjig, K. (2010). Influence of operational parameters on the decolorization of an azo by fenton process. J. Colour Sci. Technol., 4, 105-114.

[7] Crini, G. (2006). Non-conventional low-cost adsorbents for Dye removal: A review. Bioresour Technol., 9, 1061-1085.

[8] Gupta, V.K. (2009). Application of low-cost adsorbents for Dye removal–a review. J. Environ Manage, 90, 2313-2342.

[9] Robinson, T., Chandran, B. and Nigam, P. (2002). Removal of Dyes from an artificial textile Dye effluent by two agricultural waste residues. Environ Int., 28, 29-33.

[10] Van de Ven, T.G.M., Saint-Cyr, K. and Allix, M. (2007). Adsorption of toluidine blue on pulp fibres. Colloids Surf A Physicochem. Eng. Asp, 294, 1-7.

[11] Yuan, T.Q. and Sun, R.C. (2010). Modification of straw for activated carbon preparation and application for the removal of Dyes from aqueous solutions, in cereal straw as a resource for sustainable biomaterials and biofuels, ed Amsterdam: Elsevier, 239-252.

[12] Matsui, Y. Ando, N. Yoshida, T. Kurotobi, R. Matsushita, T. and Ohno, K. (2011). Modelling high adsorption capacity and kinetics of organic macromolecules on super-powdered activated carbon. Water Res., 45, 1720-1728.

[13] Toor, M. and Jin, B. (2012). Adsorption characteristics, isotherm, kinetics, and diffusion of modified natural bentonite for removing diazo Dye. Chem. Eng. J., 187, 79-88.

[14] Gautam, P. Madathil, D. Brijesh Nair, A.N. (2013). Nanotechnology in Waste Water Treatment: A Review. Int. J. Chem. Tech. Res., 5, 2303-2308.

[15] Iijima, S. (1991). Helical Microtubules of Graphitic Carbon. Nature, 354, 56-58.

[16] Rubio, A., Corkill, J.L., Cohen, M.L. (1994). Theory of graphitic boron nitride nanotubes. Physical Review B, 49, 5081-5084.

[17] Chopra, N.G., Luyken, R.J., Cherrey, K., Crespi, V.H., Cohen, M.L., Louie, S.G. (1995). Boron nitride nanotubes. Science, 269, 966–967.

[18] Kaur, J., Singla, P., Goe, N. (2015). Adsorption of oxazole and isoxazole on BNNT surface: A DFT study. Appl. Surf. Sci., 328, 632-640.

[19] Azarakhshi, F., Nori-Shargh, D., Attar, H., Masnabadi, N., Yahyaei, H., Mousavi N. and Boggs, E. (2011). Conformational behaviours of 2-substituted cyclohexanones: A complete basis set, hybrid-DFT study and NBO interpretation. Mol. Simul., 37(14), 1207-1220.

[20] Azarakhshi, F., Nori-Shargh, H., Masnabadi, N., Yahyaei, H., Mousavi, N. (2012). Conformational behaviours of 2-Substituted Cyclohexanone Oximes: An Ab Initio, Hybrid DFT study, and NBO interpretation. Azo Silicon Relat. Elem., 187, 276-293.

[21] Peyghan, A.A., Noei, M., Yourdkhani, S. (2013). Al-doped graphene-like BN nanosheet as a sensor

for para-nitrophenol: DFT study. Superlattices Microstruct., 59, 115–122.

[22] Beheshtian, J., Peyghan, A.A., Tabar, M.B., Bagheri, Z. (2013). DFT study on the functionalization of BN nanotubes with sulfamide. Appl. Surf. Sci., 266, 182–187.

[23] Farmanzadeh, D. & Ghazanfary, S. (2014). Interaction of vitamins A, B1, C, B3 and D with zigzag and armchair boron nitride nanotubes: a DFT study. C. R. Chim., 17, 985–993.

[24] Peyghan, A.A., Soltani, A., Pahlevani, A.A., Kanani, Y., Khajeh, S. (2013). A first-principles study of the adsorption behaviour of CO on Al- and Ga-doped single-walled BN nanotubes. Appl. Surf. Sci., 270, 25–32.

[25] Soltania, A., Ahmadianb, N., Amirazamic, A., Masoodia, A., Lemeskic, E.T., Moradi, A.V., (2012). Theoretical investigation of OCN-adsorption onto boron nitride nano-tubes. Appl. Surf. Sci., 261, 262–267.

[26] Sundaram, S., Jayaprakasam, R., Dhandapani, M., Senthil, T.S., Vijayakumar, V.N. (2017). Theoretical (DFT) and experimental studies on multiple hydrogen bonded liquid crystals comprising between aliphatic and aromatic acids. J Mol. Liq. 243, 14–21.

[27] Glendening, E.D., Badenhoop, J.K., Reed, A.E., Carpenter, J.E., Bohmann, J.A., Morales, C.M. (2004). Theoretical Chemistry Institute, University of Wisconsin, Madison, WI, NBO Version 5.G.

[28] Seminario, J.M. & Politzer, P. Eds. (1995). Modern Density Function Theory, a Tool for Chemistry, 53. Elsevier, Amsterdam.

[29] Frisch, M.J., Trucks, G.W., Schlegel, H.B., Scuseria, G.E., Robb, M.A., Cheeseman, J.R., Scalmani, G., Barone, V., Mennucci, B., Petersson, G.A., Nakatsuji, H., Caricato, M., Li, X. et al., (2009). Gaussian 09, Revision A.02 (Gaussian Inc., Wallingford, CT).

[30] Frisch, A., Nielson, A.B. and Holder, A.J. (2000). Gauss View User Manual (Gaussian Inc., Pittsburgh, PA).

[31] Azarakhshi, F., Khaleghian, M. and Farhadyar, N. DFT study and NBO analysis of conformational properties of 2-Substituted 2-Oxo-1, 3, 2-dioxaphosphorinanes and their dithia and diselena analogs. (2015). Lett. Org. Chem., 12, 516-522.

[32] Sheikhi, M., Shahab, S., Filippovich, L., Dikusar, E. and Khaleghian, M. (2018). DFT investigations (geometry optimization, UV/Vis, FT-IR, NMR, HOMO-LUMO, FMO, MEP, NBO, Excited States) and the syntheses of new pyrimidine dyes.Chin. J. Struct. Chem., 37, 1201-1222.

AUTHORS BIOSKETCHES

Toba Mansori, M.Sc., Department of Chemistry, Varamin-Pishva Branch, Islamic Azad University, Varamin, Iran

Nazanin Farhadyar, Associate Professor, Department of Chemistry, Varamin-Pishva Branch, Islamic Azad University, Varamin, Iran, *Email: diamond4far@gmail.com*

Fatemeh Azarakhshi, Assistant Professor, Department of Chemistry, Varamin-Pishva Branch, Islamic Azad University, Varamin, Iran, *Email: fa_azarakhshi@yahoo.com*